

Theoretical Studies on the Photochemistry of the Cis-to-Trans Conversion in Dinuclear Gold Halide Bis(diphenylphosphino)ethylene Complexes[†]

Peter Schwerdtfeger,* Alice E. Bruce, and Mitchell R. M. Bruce

Contribution from the Department of Chemistry, University of Auckland, Private Bag 92019, Auckland, New Zealand, and the Department of Chemistry, University of Maine, Orono, Maine 04469

Received October 29, 1997. Revised Manuscript Received March 31, 1998

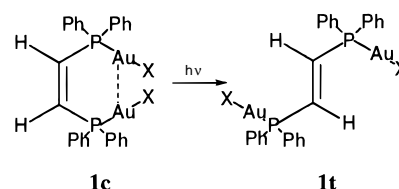
Abstract: Ab initio calculations were carried out on *cis*- and *trans*-(diphosphino)ethylene digold halide, Au₂X₂C₂H₂(PH₂)₂ (X = Cl, Br, I), the model compounds for dinuclear gold(I) bis(diphenylphosphino)ethylene complexes, Au₂X₂(dppee). The calculations reveal aurophilic interactions in the *cis* compound, thus stabilizing the *cis* complex with respect to the *trans* species. The aurophilic interaction, caused by an interplay between relativistic and electron correlation effects, increases with increasing softness of the ligand attached to gold. Excited-state calculations show ethylene π* contributions only for the *cis* compound, but not for the *trans* compound, thus explaining why the *trans* complex does not isomerize to the *cis* compound upon UV radiation at wavelengths greater than 220 nm. The singlet excitation can be best described as a charge-transfer transition from the halogen lone pair to the Au (5d6s6p) orbitals with strong intermixing from phosphorus (sp) orbitals. Because of symmetry reasons, these orbitals mix with the ethylene C=C π* orbital for the *cis* compound. As a result, the aurophilic interaction causes a stabilization of the first excited singlet state. This causes a red shift in the spectrum of the *cis* isomers relative to the *trans* isomers, which increases with decreasing Au–Au bond distance. The *cis* compound also shows enhanced transition probabilities compared to the *trans* compound for the first electronic singlet excitation. Nonrelativistic calculations reveal only a weak bond between the C₂H₂(PH₂)₂ unit and Au₂Cl₂. The calculated Au–Au distances in Au₂X₂ decrease from X = F down the group to X = I. This contrasts with the increasing Au–X bond distance when going to the heavier halides and indicates an aurophilic attraction.

I. Introduction

It is well-known that several gold phosphine complexes exhibit excited-state luminescence, which is of current interest in the development of photochemical switches.¹ A very recent example is the unusual solvent-stimulated yellow luminescence of supramolecular Au₃(CH₃N=COCH₃)₃ discovered by the research group of A. L. Balch.² A common characteristic of these compounds is that they form aurophilic interactions. The photochemical activity is, however, not understood; the emissions from metal-centered transitions.³ Some of these gold compounds also have unusual nonlinear optical properties, as a recently published paper by Xin et al. on [MAu₂S₄](AsPh₃)₂ (M = Mo or W) shows.⁴

In a recent paper, Foley et al.⁵ investigated the photochemical *cis*-to-*trans* conversion in dinuclear gold(I) bis(diphenylphos-

phino)ethylene complexes, Au₂X₂(dppee) (X = Cl, Br, I, *p*-SC₆H₄CH₃),



We summarize the following observations for this photochemical process:⁵

(i) The uncoordinated *cis*- and *trans*-dppee ligand shows a broad UV absorption band around $\lambda_{\text{max}} = 260$ nm. Both the *cis* and *trans* species have similar molar absorptivity and do not isomerize from *cis* to *trans* or vice versa under the applied conditions.

(ii) The visible spectra of **1c** and **1t** show red shifts for softer X ligands.

(iii) In contrast to the uncoordinated species, **1c** isomerizes irreversibly to **1t**; i.e., irradiation of **1t** does not produce a detectable amount of **1c**.

It is clear that coordination of AuX to dppee is responsible for the observed photochemical isomerization. It is, however, not obvious if the thermodynamic stability of the two isomers, which may be influenced by aurophilic interactions in **1c**, and/or the nature of the excited electronic state (e.g., C=C π* contributions) is responsible for this irreversible isomerization.

[†] Dedicated to Prof. W. R. Roper (Auckland) on the occasion of his 60th birthday.

(1) (a) Tzeng, B.-C.; Chan, C.-K.; Cheung, K.-K.; Che, C.-M.; Peng, S.-M. *J. Chem. Soc., Chem. Commun.* **1997**, 135. (b) Balch, A. L.; Calalano, V. J.; Olmstead, M. M. *Inorg. Chem.* **1990**, *29*, 585. (c) Forward, J. M.; Bohmann, D.; Fackler, J. P., Jr.; Staples, R. J. *Inorg. Chem.* **1995**, *34*, 6330.

(2) (a) Vickery, J. C.; Olmstead, M. M.; Fung, E. Y.; Balch, A. L. *Angew. Chem., Int. Ed. Engl.* **1997**, *36*, 1179; *Angew. Chem.* **1997**, *109*, 1227. (b) Gade, L. H. *Angew. Chem., Int. Ed. Engl.* **1997**, *36*, 1171; *Angew. Chem.* **1997**, *109*, 1219.

(3) McCleskey, T. M.; Gray, H. B. *Inorg. Chem.* **1992**, *31*, 1733.

(4) Zheng, He-gen; Ji, Wei; Low, M. L. K.; Sakane, G.; Shibahara, T.; Xin, Xin-quan. *J. Chem. Soc., Dalton Trans.* **1997**, 2357.

(5) Foley, J. B.; Bruce, A. E.; Bruce, M. R. M. *J. Am. Chem. Soc.* **1995**, *117*, 9596.

We therefore decided to study the model compound $\text{Au}_2\text{X}_2\text{C}_2\text{H}_2(\text{PH}_2)_2$ by theoretical methods.

In a series of papers on the structure and stability of gold compounds, it was shown that relativistic effects dominate the chemistry and physics of gold compounds;^{6,7} cf., see the review article by Pyykkö.⁸ Pyykkö also showed that aurophilic interactions are caused by relativistic effects together with dispersive interactions.^{9–11} Aurophilic attractions can be as large as 30–50 kJ/mol and therefore belong to the group of strong dispersive interactions.¹¹ The Au–Au bond distance in compounds showing aurophilic interactions ranges from 2.8 Å, for the strong Au–Au interactions with Au connected to soft ligands, to >3.5 Å for the weak interactions. The small measured Au–Au distance of 3.05 Å in $\text{Au}_2\text{Cl}_2(\text{cis-dppe})$ ¹² indicates a strong aurophilic attraction.

The thermodynamic stability of *trans*-dppe has been calculated by semiempirical methods, and this compound is estimated to be 23 kJ/mol more stable than the corresponding *cis* isomer.⁵ Thus, relativistically enhanced aurophilic attraction between the two P–Au–X units may well overcompensate the *trans* stabilization, suggesting that the nature of the excited state is responsible for the *cis*-to-*trans* isomerization. In this case, we should expect a large C=C π^* contribution for **1c** but *not* for **1t**, which will be examined in detail.

In this article, we study the stability and photochemistry of *cis*- and *trans*- $\text{Au}_2\text{X}_2(\text{dppe})$ (X = Cl (**2**), Br (**3**), I (**4**)) by quantum theoretical methods. The electronic ground-state structures are shown in Figure 1. The computational details are described in the next section. The results and discussion are presented in section III. A summary is given in the last section.

II. Computational Details

It is clear that theoretical calculations of ground and excited states on compounds such as $\text{Au}_2\text{X}_2\text{C}_2\text{H}_2(\text{PPh}_2)_2$ should include both relativistic and electron correlation effects and should therefore be carried out using rather large basis sets for gold and the important ligands in order to accurately describe aurophilic interactions and excited electronic states. This is currently not feasible for any *ab initio* or density functional theory. We therefore had to introduce several assumptions and approximations.

The first assumption is that the energetics of the *cis*-to-*trans* conversion of dppe are not very sensitive to basis set effects and, therefore, rather moderate basis sets can be used for carbon, hydrogen, and phosphorus. This assumption will be tested on the uncoordinated dppe, $\text{C}_2\text{H}_2(\text{PPh}_2)_2$ (**5**), and $\text{C}_2\text{H}_2(\text{PH}_2)_2$ (**6**). Second, the excited electronic states are probably influenced by aurophilic interactions, and as a result, relativistic and electron correlation effects must be accounted for accurately. Relativistic effects will therefore be described by a scalar relativistic pseudopotential for gold,⁶ and electron correlation effects

are considered at the second-order Møller–Plesset level (MP2).¹³ Third, the phenyl ligands are substituted by a simple hydrogen atom. This may be seen as a more severe approximation, however; in coordinated $\text{Au}_2\text{X}_2\text{C}_2\text{H}_2(\text{PPh}_2)_2$, there is no (or little) interaction between the phosphorus 3p lone pair and the aromatic π electrons because of coordination to AuX. In this case, it will be interesting to compare the *cis*-to-*trans* stability of the two compounds, $\text{C}_2\text{H}_2(\text{PPh}_2)_2$ and $\text{C}_2\text{H}_2(\text{PH}_2)_2$. Fourth, distortions in the electronic excited states are not investigated. Calculations on the simple ligand **6** revealed that a complete geometry optimization of the excited singlet state to locate all important local minima is currently an impossible task at the correlated *ab initio* level. Fifth, solvent effects are neglected. The experiments have been carried out in relatively inert solvents (CHCl_3 and CH_2Cl_2),⁵ and the van der Waals interaction between the solvent molecules and $\text{Au}_2\text{X}_2\text{C}_2\text{H}_2(\text{PPh}_2)_2$ will not alter the electronic states significantly. Neglect of solvent effects is expected to lie within the error of the many approximations applied to our systems. Finally, the ligands X = Cl, Br, and I are used for all calculations.

The differences in stability between the isomers of $\text{C}_2\text{H}_2(\text{PPh}_2)_2$ (dppe) and $\text{C}_2\text{H}_2(\text{PH}_2)_2$ are evaluated at the molecular mechanics (MM2),¹⁴ the semiempirical (AM1 and PM3),^{15–17} and the 6-31G* HF levels,^{18,19} and compared with MP2 6-31G* and 6-311++G** calculations for $\text{C}_2\text{H}_2(\text{PH}_2)_2$. At the optimized 6-31G* and 6-311++G** geometries, we performed CIS calculations (configuration interaction with single excitations only)¹⁹ on $\text{C}_2\text{H}_2(\text{PH}_2)_2$ for the first few singlet and triplet excited electronic states lying in the near-UV region. The largest oscillator strength calculated in all cases is the one for the C=C $\pi \rightarrow \pi^*$ transition (with a large admixture of phosphorus 3p orbitals), and we will therefore restrict ourselves to the discussion of the first two excited singlet states. We mention that a number of triplet states are lying below the first excited singlet state at the CIS level. CI with single excitations only is, however, not a very accurate method for excited states but is useful for discussing qualitative trends and for the determination of important configurations. The CIS results were thus used for the construction of the CAS (complete active space) for subsequent MP2 calculations (selected MP2 starting from localized CASSCF orbitals), denoted as CAS-LMP2 for this paper.²⁰ For the first excited singlet and triplet states, we also performed 6-31+G* calculations to determine the P–C–C–P torsion angle potential curve for $\text{C}_2\text{H}_2(\text{PH}_2)_2$ at the CAS-LMP2 level (for the singlet state) and the single-reference MP2 level (for the triplet state).

The $\text{Au}_2\text{X}_2\text{C}_2\text{H}_2(\text{PH}_2)_2$ compounds (X = Cl (**2**), Br (**3**), I (**4**)) were preoptimized at the pseudopotential (PP) Hartree–Fock level using Hay–Wadt relativistic PPs and basis sets²¹ (LANL1MB)¹⁹ and further refined by MP2 LANL1DZ¹⁹ calculations. We chose three different geometries: (a) the *trans* geometry (assuming that rotation around the C–P axis will not lead to large changes in the total energy), (b) the *cis* geometry allowing for interactions between the gold atoms, (c) the *cis* geometry where a rotation around the C–P axis prohibits aurophilic interactions. Frequency analyses confirmed that these geometries

(13) Møller, C.; Plesset, M. S. *J. Chem. Phys.* **1934**, *46*, 618.

(14) Burkert, U.; Allinger, N. L. *Molecular Mechanics*; ACS Monograph 177; American Chemical Society: Washington, DC, 1982.

(15) (a) Dewar, M. J. S.; Zoebisch, E. G.; Healy, E. F. *J. Am. Chem. Soc.* **1985**, *107*, 3902. (b) Dewar, M. J. S.; Reynolds, C. H. *J. Comput. Chem.* **1986**, *2*, 140.

(16) (a) Stewart, J. J. P. *J. Comput. Chem.* **1989**, *10*, 209. (b) Stewart, J. J. P. *J. Comput. Chem.* **1989**, *10*, 221.

(17) Program CHEM3D, Version 3.5, CambridgeSoft Corporation, Cambridge, MA, 1996.

(18) Ditchfield, R.; Hehre, W. J.; Pople, J. A. *J. Chem. Phys.* **1971**, *54*, 724.

(19) Frisch, M. J.; Trucks, G. W.; Schlegel, H. B.; Gill, P. M. W.; Johnson, B. G.; Robb, M. A.; Cheeseman, J. R.; Keith, T.; Petersson, G. A.; Montgomery, J. A.; Raghavachari, K.; Al-Laham, M. A.; Zakrzewski, V. G.; Ortiz, J. V.; Foresman, J. B.; Cioslowski, J.; Stefanov, B. B.; Nanayakkara, A.; Challacombe, M.; Peng, C. Y.; Ayala, P. Y.; Chen, W.; Wong, M. W.; Andres, J. L.; Replogle, E. S.; Gomperts, R.; Martin, R. L.; Fox, D. J.; Binkley, J. S.; DeFrees, D. J.; Baker, J.; Stewart, J. J. P.; Head-Gordon, M.; Gonzalez, C.; Pople, J. A. *GAUSSIAN94*, Rev. D.3; Gaussian, Inc.: Pittsburgh, PA, 1996.

(20) McDouall, J. J.; Peasley, K.; Robb, M. A. *Chem. Phys. Lett.* **1988**, *148*, 183.

(21) Hay, P. J.; Wadt, W. R. *J. Chem. Phys.* **1985**, *82*, 299.

(6) (a) Schwerdtfeger, P.; Dolg, M.; Schwarz, W. H. E.; Bowmaker, G. A.; Boyd, P. D. W. *J. Chem. Phys.* **1989**, *91*, 1762.

(7) (a) Schwerdtfeger, P. *J. Am. Chem. Soc.* **1989**, *111*, 7261. (b) Schwerdtfeger, P.; Boyd, P. D. W.; Burrell, A. K.; Robinson, W. T.; Taylor, M. J. *Inorg. Chem.* **1990**, *29*, 3593. (c) Schwerdtfeger, P.; Dolg, M. *Phys. Rev. A* **1991**, *43*, 1644. (d) Schwerdtfeger, P.; Boyd, P. D. W.; Brienne, S.; Burrell, A. K. *Inorg. Chem.* **1992**, *31*, 3411. (e) Schwerdtfeger, P.; Bowmaker, G. A. *J. Chem. Phys.* **1994**, *100*, 4487. (f) Antes, L.; Dapprich, S.; Frenking, G.; Schwerdtfeger, P. *Inorg. Chem.* **1996**, *35*, 2089.

(8) Pyykkö, P. *Chem. Rev.* **1988**, *88*, 563.

(9) (a) Pyykkö, P.; Li, J.; Runeberg, N. *Chem. Phys. Lett.* **1994**, *218*, 133. (b) Pyykkö, P.; Zhao, Y.-F. *Angew. Chem., Int. Ed. Engl.* **1991**, *30*, 604; *Angew. Chem.* **1991**, *103*, 622. (c) Li, J.; Pyykkö, P. *Chem. Phys. Lett.* **1992**, *197*, 586. (d) Pyykkö, P.; Schneider, W.; Bauer, A.; Bayler, A.; Schmidbaur, H. *Chem. Commun.* **1997**, 1111.

(10) Pyykkö P. *Chem. Rev.* **1997**, *97*, 597.

(11) (a) Pyykkö, P.; Runeberg, N.; Mendizabal, F. *Chem. Eur. J.* **1997**, *3*, 1451. (b) Pyykkö, P.; Mendizabal, F. *Chem. Eur. J.* **1997**, *3*, 1458.

(12) Jones, P. G. *Acta Crystallogr.* **1980**, *B36*, 2775.

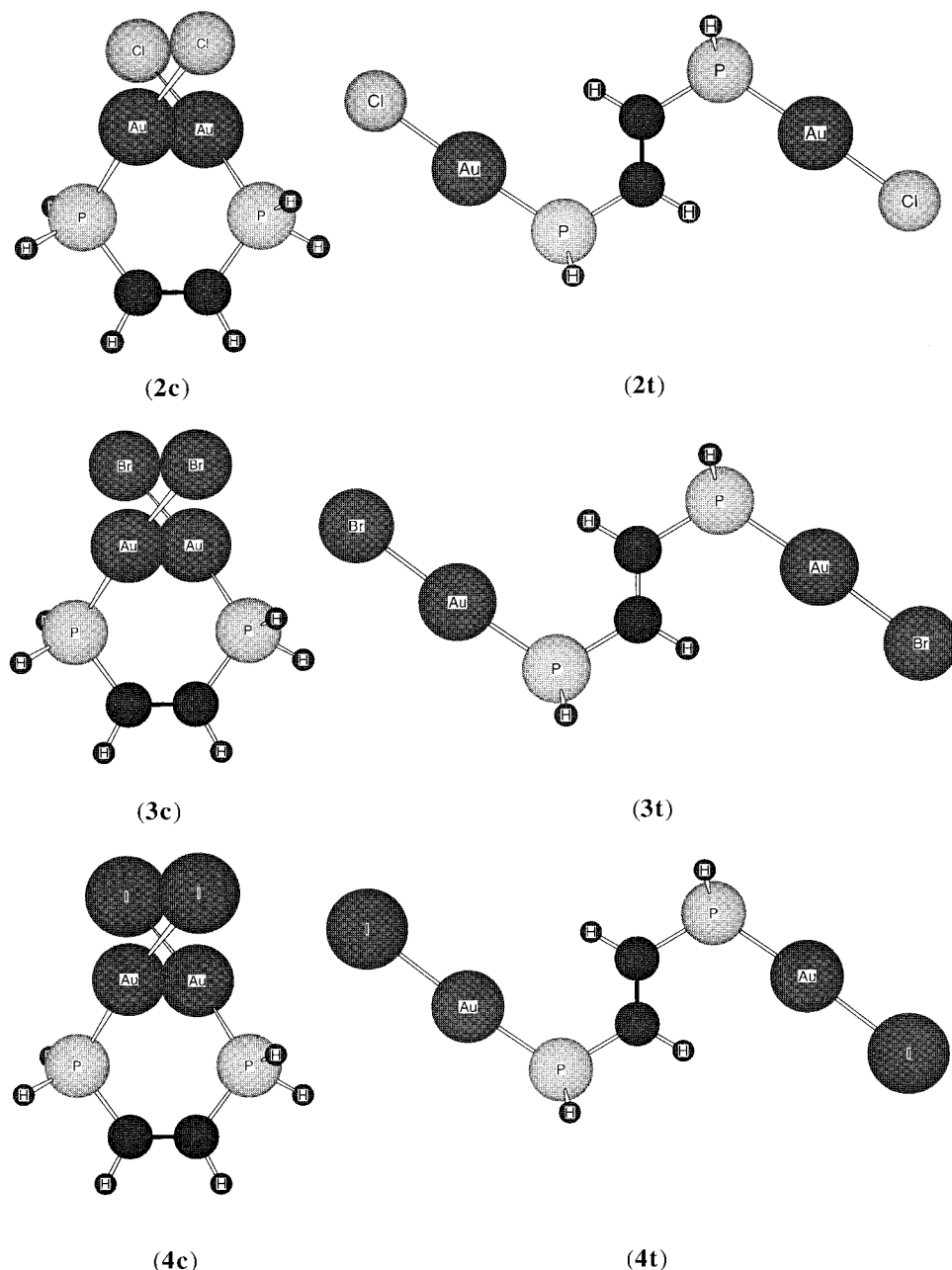


Figure 1. Optimized MP2 structures for $\text{Au}_2\text{X}_2\text{C}_2\text{H}_2(\text{PH}_2)_2$ ($\text{X} = \text{Cl}, \text{Br}, \text{I}$).

belong to local minima on the potential energy surface. Starting from these optimized MP2 geometries, we performed large-scale MP2 optimizations for structures 2–4 using the Stuttgart PPs for gold, bromine, and iodine.⁶ The six different optimized cis and trans geometries (denoted as **c** and **t**, respectively) are shown in Figure 1 (structures **2c**, **2t**, **3c**, **3t** and **4c**, **4t**).

To investigate the nature of the aurophilic interaction, we performed nonrelativistic MP2 calculations using a nonrelativistic pseudopotential and basis set for gold⁶ and relativistic HF calculations for $\text{Au}_2\text{Cl}_2\text{C}_2\text{H}_2(\text{PH}_2)_2$ (**2c'** and **2c''**, respectively). The accuracy of the pseudopotential approximation has been discussed recently in some detail.²² The pseudopotentials used here are small core pseudopotentials ($5s^25p^6-5d^{10}6s^1$ valence space for gold and valence s^2p^5 for bromine and iodine) and should be of comparable accuracy to scalar relativistic all-electron calculations. The basis sets used are as follows: For C, H, P, and Cl, we used a 6-31G* basis set. For Au, we used a contracted relativistic

($8s6p5d$)/($7s/3p/4d$) and a nonrelativistic ($9s6p5d$)/($8s/3p/4d$) basis set.⁶ For bromine and iodine, we used a ($6s6p1d$)/($5s/5p/1d$) basis set.⁶ This results in 340 primitive Gaussians contracted to 198 basis functions for $\text{Au}_2\text{Br}_2\text{C}_2\text{H}_2(\text{PH}_2)_2$, which is a rather large basis set for a correlated geometry optimization followed by a single-point CIS or CAS-LMP2 excited-state calculation. For instance, the geometry optimization for one compound consumed 350 h of CPU and 256 Mbyte of memory on a IBM RISC6000 590 workstation. At the optimized MP2 geometry, we performed single reference CIS as well as small CAS-LMP2 calculations to obtain the first electronic excited singlet state. The CAS included all important configurations determined by the CI coefficients of the CIS calculation. It was necessary to use different definitions of the CAS for the various compounds because of the very different nature of the excited states as indicated by the CI coefficients. For example, for the first excited singlet state of $\text{Au}_2\text{I}_2\text{C}_2\text{H}_2(\text{PH}_2)_2$, we chose 3 occupied and 3 unoccupied orbitals, resulting in 210 configuration-state functions (CSF) followed by a selected MP2 calculation. The CAS calculations were often very difficult to converge to a change in the total electronic energy of $<10^{-8}$ au and were therefore very demanding in computer time. We only succeeded in obtaining a CAS-

(22) (a) Schwerdtfeger, P.; Fischer, T.; Dolg, M.; Igel-Mann, G.; Nicklass, A.; Stoll, H.; Haaland, A. *J. Chem. Phys.* **1995**, *102*, 2050. (b) Leininger, T.; Nicklass, A.; Stoll, H.; Dolg, M.; Schwerdtfeger, P. *J. Chem. Phys.* **1996**, *105*, 1052.

Table 1. Selected Torsion Angles and Relative Stabilities of the Cis and Trans Isomers of dppee (**5**) and C₂H₂(PH₂)₂ (**6**) at the MM2, PM3, AM1, HF, and MP2 Levels^a

property	MM2	AM1	PM3	6-31G*/HF	6-31G*/MP2	6-311++G**/MP2
<i>trans</i> -dppee, 5t						
P-C-C-P	177.2	176.6	172.7	177.2		
C _{ph} -P-C-C	171.7	127.3	157.8	128.4		
C' _{ph} -P-C-C	-89.4	20.5	51.6	-126.7		
C-C-P-C _{ph}	-174.5	151.4	-170.9	128.4		
C-C-P-C' _{ph}	-75.3	-103.4	85.2	-126.7		
<i>cis</i> -dppee, 5c						
P-C-C-P	0.0	2.2	2.7	3.6		
C _{ph} -P-C-C	85.4	148.7	143.5	130.9		
C' _{ph} -P-C-C	-174.8	-106.3	-112.4	-124.5		
C-C-P-C _{ph}	-85.3	144.2	143.5	131.0		
C-C-P-C' _{ph}	-169.7	-110.5	-112.4	-124.5		
ΔE	0.2	9.3	23.3	13.7		
<i>cis</i> -dppee, 5c'						
P-C-C-P	2.0	0.0	0.0	0.0		
C _{ph} -P-C-C	-62.0	126.2	108.4	123.2		
C' _{ph} -P-C-C	-161.7	-128.8	-147.3	-132.4		
C-C-P-C _{ph}	-69.2	128.8	147.3	132.3		
C-C-P-C' _{ph}	-169.7	-126.3	-108.4	-123.4		
ΔE	9.0	10.4	27.5	16.1		
<i>trans</i> -C ₂ H ₂ (PH ₂) ₂ , 6t						
P-C-C-P	180.0	180.0	180.0	180.0	180.0	180.0
H _p -P-C-C	-128.0	132.7	128.8	112.5	115.0	117.3
H' _p -P-C-C	130.8	33.7	28.4	15.2	18.2	21.2
C-C-P-H _p	128.7	-133.3	-128.5	-112.5	-115.0	-117.3
C-C-P-H' _p	-130.2	-34.2	-28.0	-15.2	-18.2	-21.2
<i>cis</i> -C ₂ H ₂ (PH ₂) ₂ , 6c						
P-C-C-P	0.0	12.0	13.0	7.9	10.0	0.0
C _p -P-C-C	51.0	-63.2	-44.3	-42.8	-49.3	-47.7
C' _p -P-C-C	-51.0	-161.3	-144.3	-139.8	-146.0	-143.9
C-C-P-H _p	51.0	-62.9	-43.8	44.2	-49.3	-47.7
C-C-P-H' _p	-51.0	-160.9	-143.8	137.6	-146.0	-143.9
ΔE	4.5	15.8	15.8	7.4	1.7	1.8
<i>cis</i> -C ₂ H ₂ (PH ₂) ₂ , 6c'						
P-C-C-P	0.0	0.0	0.0	0.0	0.0	12.3
H _p -P-C-C	65.2	50.8	35.7	48.3	46.3	45.3
H' _p -P-C-C	166.3	148.9	135.6	142.0	143.2	141.6
C-C-P-H _p	166.4	210.9	-135.9	-38.4	-46.4	-45.4
C-C-P-H' _p	-92.5	-51.0	-35.9	-135.7	-143.3	-141.7
ΔE	5.2	20.0	15.1	17.3	4.2	4.9

^a Angles in deg and energy differences in kJ/mol. The trans compound is thermodynamically the most stable isomer and is chosen as ΔE = 0 kJ/mol. C_{ph} denotes the carbon of the phenyl group attached to phosphorus. H_p indicates the hydrogen attached to phosphorus. The prime denotes the second C_{ph} or H_p attached to phosphorus. The optimized structures are shown in Figures 2 and 3.

LMP2 value for the second excited singlet state of *cis*-Au₂Cl₂C₂H₂(PH₂)₂ and therefore only report CIS values for the first three excited singlet states.

In a previous paper, it was found that the Au-P bond is relativistically stabilized in the dinuclear complex Au₂(PH₃)₂.²³ The stabilities of the complexes have therefore been evaluated at the MP2 level using the following decomposition reaction:



trans-C₂H₂PH₂ is used for reaction 1 in all cases. We also considered the stability of Au₂X₂ by studying the decomposition reaction



There is little known about the gas-phase properties of gold halides. These compounds are also interesting for the study of ligand dependencies in aurophilic interactions. We therefore performed harmonic frequency calculations at the MP2 level for Au₂Cl₂, Au₂Br₂, and Au₂I₂ (Au₂F₂ has been studied previously).²⁴

The density plots were performed using the program MOLDEN3.2.²⁵ The plotted structures are obtained from the program package CHEM3D.¹⁷

III. Results and Discussion

Structures of dppee and C₂H₂(PH₂)₂. The results of the dppee (structures **5t**, **5c**, and **5c'**) and C₂H₂(PH₂)₂ (structures **6t**, **6t'**, **6c**, and **6c'**) calculations are summarized in Table 1 (only the important torsion angles are listed). The optimized structures are shown in Figures 2 and 3. The cis and trans structures shown are the lowest energy structures obtained from a geometry optimization. For C₂H₂(PH₂)₂ and dppee, there are several other local minima usually close in energy representing rotomers for the rotation around the C-P and P-L axes. For example, a local minimum for dppee with close contacts between two phenyl rings was found which lies quite high in energy (43.2 kJ/mol above the global minimum at the PM3 level). The different trans rotomers differ only by a few kilojoules/mole from each other. As expected, the trans structure represents the global minimum (with few exceptions,²⁶ *trans*-ethylene derivatives, C₂H₂X₂, are lower in energy than the corresponding cis compounds). For dppee, the trans structure is 14 kJ/mol more stable than the cis structure at the Hartree-Fock 6-31G*

(23) Schwerdtfeger, P.; Boyd, P. D. W. *Inorg. Chem.* **1992**, *31*, 327.

(24) Schwerdtfeger, P.; McFeaters, J. S.; Liddell, M. J.; Hrusak, J.; Schwarz, H. J. *Chem. Phys.* **1995**, *103*, 245.

(25) Schaftenaar, G. *Molden3.2*; CAOS/CAMM Center: Nijmegen, 1991.

(26) (a) Waldron, J. T.; Snyder, W. H. *J. Am. Chem. Soc.* **1973**, *95*, 5491. (b) Bowen, J. P.; Reddy, V. V.; Patterson, D. G.; Allinger, N. L. *J. Org. Chem.* **1988**, *53*, 5471. (c) Pappalardo, R. R.; Martinez, J. M.; Marcos, E. S. *Chem. Phys. Lett.* **1994**, *225*, 202.

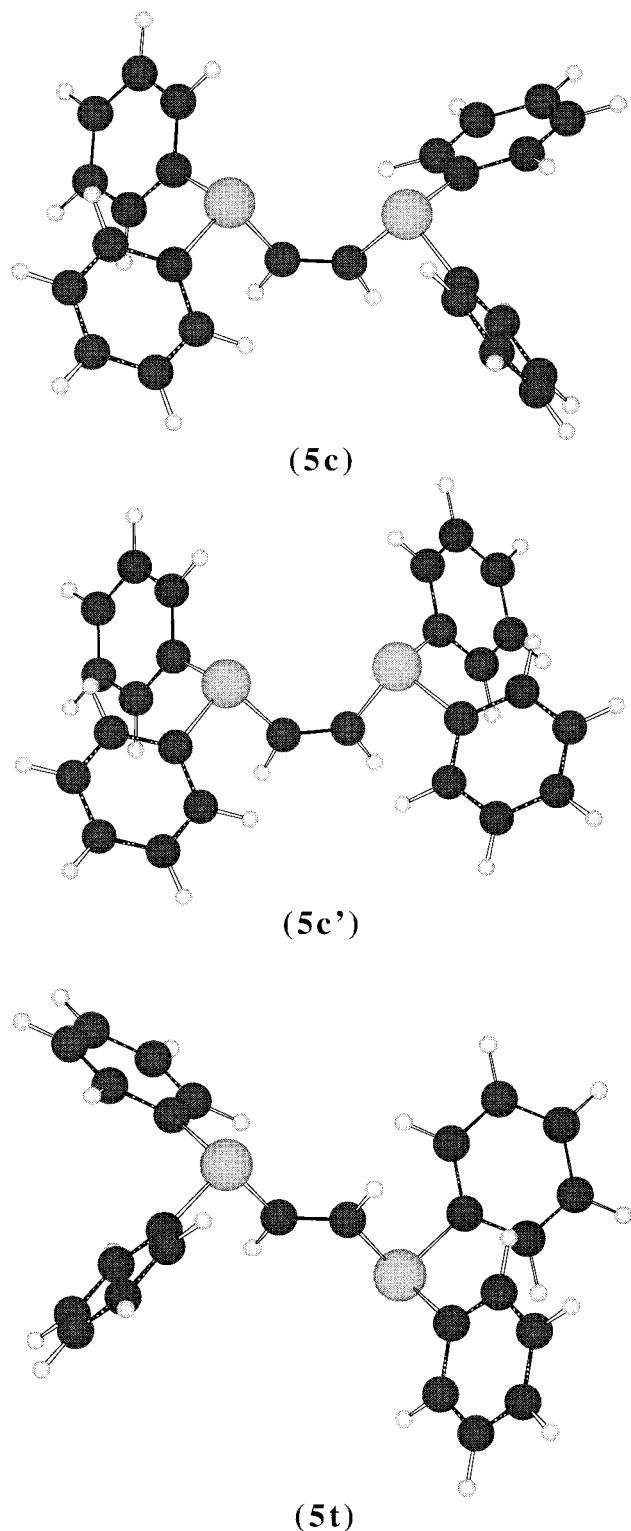


Figure 2. Optimized HF 6-31G* structures for dppee. See Table 1 for the torsion angles.

level. However, Table 1 shows that electron correlation effects are more significant than basis set effects; i.e., for $C_2H_2(PH_2)_2$, the cis-to-trans energy difference is lowered from 7.4 (HF/6-31G*) to 1.7 kJ/mol (MP2/6-31G*). Improvement of the basis set (MP2/6-311++G**) increases this difference by only 0.1 kJ/mol. This gives confidence in the accuracy of the basis sets applied in $Au_2X_2C_2H_2(PPh_2)_2$. It also suggests that the cis-to-trans energy difference in dppee is probably below 10 kJ/mol. We note that MM2 and AM1 predict this; however, the PM3

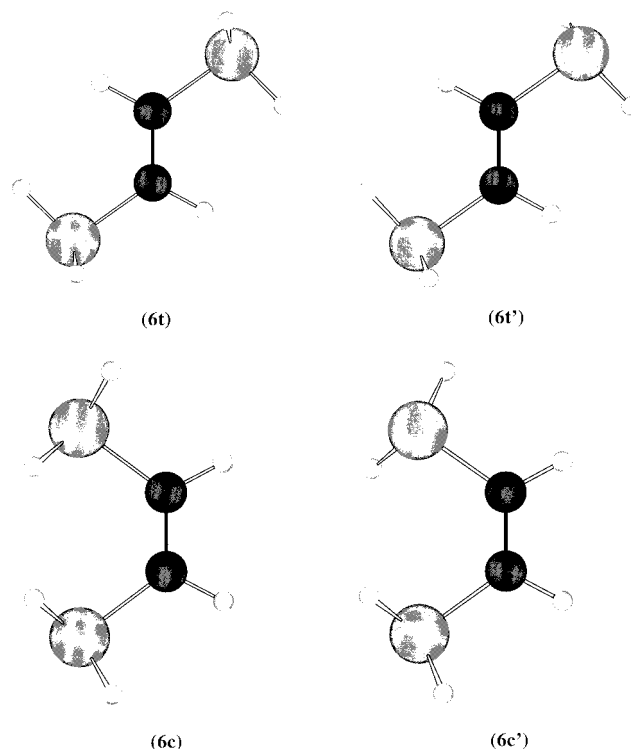


Figure 3. Optimized MP2 6-311++G** structures for $C_2H_2(PH_2)_2$. See Table 1 for the torsion angles.

results probably overestimate this energy difference. At a Au–Au distance of 3.05 Å or less, auriphilic interactions are expected to be around 30 kJ/mol.¹⁰ This is larger than the cis-to-trans energy difference. Hence, we expect that *cis*- $Au_2X_2C_2H_2(PPh_2)_2$ is thermodynamically more stable than the trans product.

The different approximations used all give reasonable results for bond distances and bond angles. However, the torsion angles can deviate substantially between the different methods applied. While PM3 is in reasonable agreement with the ab initio results, MM2 deviates substantially from the MP2-calculated torsion angles. We also note that the PCCP torsion angle is not always 180° (for the trans structure) or 0° (for the cis structure).

Excited-State Calculations for dppee and $C_2H_2(PH_2)_2$. Ethylene has its absorption peak at 162 nm.²⁷ We expect $C_2H_2(PH_2)_2$ to absorb at a longer wavelength as a result of lone-pair interaction of the P atom with the C=C π electrons. At the best level of theory (CAS-LMP2), we predict that the first excited singlet state in $C_2H_2(PH_2)_2$ occurs at ca. 200 nm (see Table 2). Analysis of the CI coefficients shows that the first singlet transition can be best described as an ethylene $\pi \rightarrow \pi^*$ transition with large admixture from the P lone pair. A comparison between the different methods shows that the 6-31G* basis set probably overestimates the singlet excitation energy as expected (excited electronic states are more sensitive to basis set effects). The CIS and CAS-LMP2 results are, however, quite comparable for $C_2H_2(PH_2)_2$.

To study the structure of $C_2H_2(PH_2)_2$ in the first excited state, we carried out calculations for $C_2H_2(PH_2)_2$ at different P–C=C–P torsion angles, τ , keeping all other internal coordinates fixed, Figure 4. This clearly shows that for both the first excited singlet and triplet state, the minimum structure is expected near $\tau = 90^\circ$. This is what we expect from a $\pi \rightarrow \pi^*$ transition. Interestingly, the triplet potential energy surface (PES) intersects the singlet ground-state PES, which, however,

(27) Wilkinson, P. G. *J. Mol. Spectrosc.* **1961**, *6*, 57.

Table 2. First Two Singlet Vertical Excitation Energies for dppee and $C_2H_2(PH_2)_2^a$

method	5, 6t	5, 6c	5, 6c'
<i>dppee</i>			
CIS/6-31G*	205 (203)	215 (204)	210 (206)
$C_2H_2(PH_2)_2$			
CIS/6-31G*	187 (174)	195 (171)	188 (181)
CIS/6-311++G**	207 (192)	209 (198)	207 (199)
CASSCF/6-31G*	172	172	170
CAS-LMP2/6-31G*	183	199	186
CASSCF/6-311++G**	210	226	226
CAS-LMP2/6-311++G**	191	208	189

^a All values are given in nm (10^{-9} m). The first singlet excitation is mainly of C=C $\pi \rightarrow \pi^*$ character with substantial 3p contributions from the phosphorus atom. At the CIS level, the second singlet excitation is given in parentheses. All calculations are carried out at the optimized 6-31G* or 6-311++G** MP2 structure. For the optimized structures, see Figures 2 and 3 (6-31G* HF only for dppee).

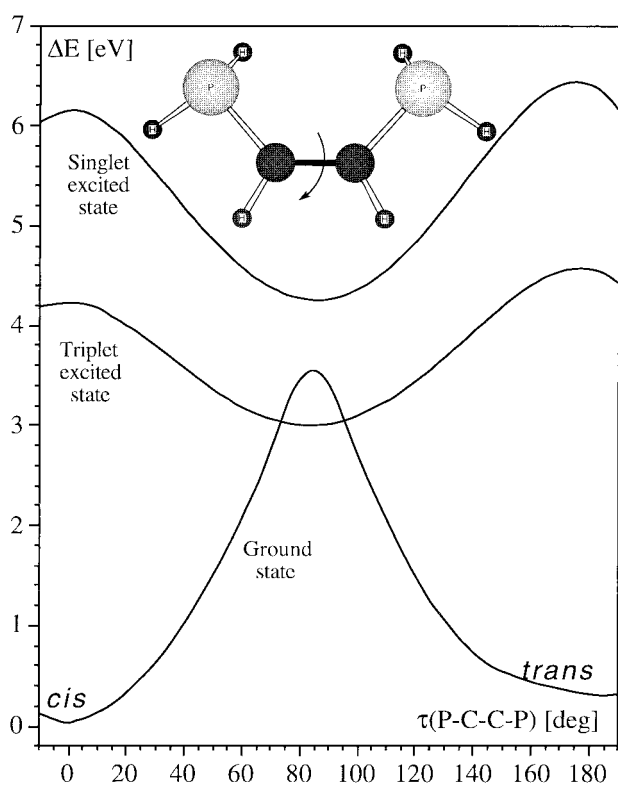


Figure 4. Ground- and excited-state potential curves ($V(\tau)$) for $C_2H_2(PH_2)_2$ leaving all other internal coordinates fixed. The singlet ground and first excited triplet states are obtained from single-reference MP2 calculations, the first excited singlet state from CAS-LMP2 calculations. Note that the calculations start from the optimized *cis* structure; hence, the *trans* structure is not optimized and therefore lies higher in energy.

could be due to the single-reference MP2 procedure applied. We note that the CAS-LMP2 calculations for the first excited singlet state were difficult to carry out near $\tau = 90^\circ$ because of convergence difficulties. A different choice of the active space did not improve the situation. As a result, we had to use a fit procedure in order to obtain the singlet excited potential curve in the region between $\tau = 80^\circ$ and 100° . Finally, we note that such a potential curve as shown in Figure 4 would lead to the expected *cis* \leftrightarrow *trans* conversion upon UV irradiation of $C_2H_2(PH_2)_2$ at around 200 nm.

The UV spectra for *cis*- and *trans*-dppee consist of a broad absorption centered at 260 nm followed by more intense absorption at lower wavelengths. The spectra show a similarity

to benzene which absorbs at 260 nm.²⁸ CIS calculations at the 6-31G* level for the HF-optimized structures of dppee give wavelengths for the first excited singlet states between 205 and 215 nm which shows the limitation of the CIS method using 6-31G* basis sets. Indeed, improving the basis sets from 6-31G* to 6-311++G** for $C_2H_2(PH_2)_2$ results in an increase of ca. 20 nm. Unfortunately, CAS-LMP2 calculations were not feasible for dppee. An analysis of the CI coefficients for dppee shows that the first excited singlet state has large ethylene π^* character. Irradiation of *cis*-dppee ($\lambda \geq 245$ nm; 4.8 mM in chloroform) does not show *cis*/*trans* conversion.⁵ The lack of photoisomerization and the similarity of the spectra to benzene suggest that the excitation occurring around 260 nm is probably a localized phenyl $\pi \rightarrow \pi^*$ transition with little ethylene π^* admixture. Nevertheless, the calculation suggests that irradiation at lower wavelengths (ca. 200 nm) will result in some *cis*-to-*trans* conversion of dppee. However, irradiation of *cis*-dppee at lower wavelengths ($\lambda \geq 210$ nm; 9 mM in acetonitrile) does not result in isomerization even after 30 min of photolysis.²⁹ The absence of photoisomerization at $\lambda \geq 210$ nm can be interpreted in several ways. (1) The ethylene $\pi \rightarrow \pi^*$ transition lies at a lower wavelength than is accessible under our experimental conditions. (2) Irradiation produces a short-lived ethylene $\pi \rightarrow \pi^*$ excited state that rapidly relaxes to the lower energy phenyl $\pi \rightarrow \pi^*$ excited state, which is not photochemically active. Rapid internal conversion from upper excited states frequently occurs for molecules in condensed media.³⁰ (3) The CIS calculations overestimate the ethylene π^* contribution to the first excited state. More accurate correlated calculations (like CASPT2) with larger basis sets may provide more insight.

Structures and Stability of $Au_2X_2C_2H_2(PH_2)_2$. The optimized geometries for $Au_2X_2C_2H_2(PH_2)_2$ ($X = Cl, Br, \text{ and } I$) are shown in Figure 1. The corresponding structural parameters are listed in Table 3. The *cis* structures clearly show auophilic interactions. The Au–Au bond distance, r_e , follows the trend 3.16 Å ($X = Cl$) > 3.11 Å ($X = Br$) > 3.06 Å ($X = I$). The experimental Au–Au bond distance in $Au_2X_2(\textit{cis}\text{-dppee})$ is 3.05 Å for $X = Cl$ ¹² and 2.95 Å for $X = I$.³¹ This indicates that our calculations underestimate the auophilic interaction most likely due to the limited basis set used and the neglect of the electronic effects from the phenyl ligands. In all cases, the *cis* structure is more stable than the *trans* structure, and therefore, the auophilic interaction is stronger than the *trans* stabilization. By comparing the energy differences (ΔE) between the *cis* and *trans* structures (Table 3), we conclude the following trend for the auophilic interaction, $Au_2I_2C_2H_2(PH_2)_2 > Au_2Br_2C_2H_2(PH_2)_2 > Au_2Cl_2C_2H_2(PH_2)_2$. Hence, soft ligands such as iodine increase the auophilic stabilization.

Perreault et al.³² showed that there is a correlation between the Au–Au distance, r_e , and the Au–Au stretching force constant, k_e , applying the Herschbach–Laurie equation,³³ thus establishing a theoretical foundation for the auophilic interaction. By using their best fit between $r_e(\text{Au–Au})$ (given in Å) and $k_e(\text{Au–Au})$ ³² and taking the spectroscopic constants for gas-

(28) Cardinal, J. R.; Mukerjee, P. *J. Phys. Chem.* **1978**, *82*, 1614.

(29) A 9 mM solution of *cis*-dppee in CH_3CN was irradiated in a quartz vessel with unfiltered light from a 300-W Hg arc lamp (Oriol). Aliquots were withdrawn at 10-min intervals, the solvent was evaporated, the residue was redissolved in CD_2Cl_2 , and the 1H NMR spectrum was recorded. No *trans*-dppee was detected after a total of 30 min of photolysis.

(30) Turro, N. J. *Modern Molecular Photochemistry*; Benjamin/Cummings: CA, 1978.

(31) Foley, J. B.; Gay, S.; Runnels, P.; Bruce, A. E.; Bruce, M. R. M.; Foxman, B.; Schwerdtfeger, P. Unpublished results.

(32) Perreault, D.; Drouin, M.; Michel, A.; Miskowski, V. M.; Schaefer, W. P.; Harvey, P. D. *Inorg. Chem.* **1992**, *31*, 695.

(33) Herschbach, D. R.; Laurie, V. W. *J. Chem. Phys.* **1961**, *35*, 458.

Table 3. Structural Parameters for Au₂X₂C₂H₂(PH₂)₂ (X = Cl, Br, I)^a

property	2			3		4	
	cis (NR)	cis	trans	cis	trans	cis	trans
distances							
Au–Au	3.304	3.158	6.929	3.111	6.929	3.062	6.938
Au–X	2.713	2.309	2.306	2.429	2.424	2.611	2.605
Au–P	4.428	2.277	2.274	2.290	2.286	2.304	2.300
C–P	1.817	1.827	1.816	1.827	1.816	1.828	1.816
C–C	1.348	1.347	1.345	1.347	1.345	1.347	1.345
C–H	1.089	1.089	1.090	1.089	1.090	1.089	1.090
P–H	1.411	1.405	1.405	1.405	1.405	1.406	1.405
X–X	4.244	5.323	10.81	5.405	10.99	5.566	11.32
angles							
C–C–P	127.5	126.2	120.9	126.5	120.8	126.6	120.7
C–C–H	117.9	118.0	120.6	117.8	120.7	117.8	120.7
C–P–H ₁	99.2	99.7	102.2	99.6	102.3	99.5	102.3
C–P–H ₂	101.9	103.7	102.2	103.7	102.3	103.5	102.3
C–P–Au	110.0	113.7	115.3	113.4	115.0	113.7	114.7
P–Au–X ₁	105.0	174.0	177.6	172.6	176.8	172.0	176.6
P–Au–X ₂	96.2	81.0		81.4		83.2	
torsion angles							
H–C–C–H	0.0	0.3	180.0	0.0	180.0	0.3	180.0
P–C–C–P	0.0	–5.0	180.0	–5.0	180.0	–4.9	180.0
C–C–P–H ₁	37.7	96.2	128.5	96.9	128.5	98.0	128.5
C–C–P–H ₂	134.9	–160.2	–128.5	–159.5	–128.5	–158.6	128.5
C–C–P–Au	70.0	–33.7	0.0	–32.8	0.0	–31.9	0.0
C–P–Au–X ₁	44.3	–19.7	0.8	–15.8	0.0	–21.9	0.0
C–P–Au–X ₂	–2.2	–75.8		–75.7		–75.0	
X–Au–Au–X	157.3	–91.4	180.0	–93.7	180.0	–93.3	180.0
energies							
ΔE(cis/trans)		–4.9	0	–7.7	0	–11.9	0
ΔU	93.2	333.4	328.5	298.7	291.0	253.7	241.8

^a Distances in Å, angles in deg, and energies in kJ/mol. ΔE(cis/trans) denotes the energy difference between the cis and trans compound, and ΔU represents the decomposition energy for reaction 1, Au₂X₂C₂H₂(PH₂)₂ → Au₂X₂ + C₂H₂PH₂. NR denotes a nonrelativistic calculation. The optimized structures are shown in Figure 1.

phase Au₂ into account,³⁴ we obtain for the Au–Au interaction energy (*D*, in kJ/mol)

$$D(\text{Au–Au}) = 1.27 \times 10^6 e^{-3.5r_e^{\text{Au–Au}}} \text{ [kJ/mol]} \quad (3)$$

For example, if we use the experimental bond distance of gas-phase Au₂ (*r*_e = 2.472 Å),³⁴ we obtain *D*(Au–Au) = 222 kJ/mol (experimental value 222 kJ/mol³⁴). For a Au–Au distance of 3.0 Å, we obtain *D*(Au–Au) = 35 kJ/mol, in very good agreement with estimated aurophilic interaction energies at such a distance.³⁵ At a distance of 3.5 Å, the aurophilic interaction is down to 6 kJ/mol. Equation 3 can be compared with a very similar formula published by Pyykkö.¹⁰ By using the recommended parameters (*a* = 2.68 Å, *b* = –29 Å, and *n* = 3.95),¹⁰ Pyykkö's formula gives *D*(Au–Au) = 224 kJ/mol at 2.472 Å, 44 kJ/mol at 3.0 Å, and 9 kJ/mol at 3.5 Å, in good agreement with our results. Differentiating eq 3 twice with respect to the distance and converting to appropriate units give

$$r_e = 3.25 - 0.29 \ln k_e \quad (4)$$

Here *r*_e(Au–Au) is given in Å and the force constant *k*_e(Au–Au) in mdyn/Å. This compares reasonably well with the fit formula given by Perreault et al.³² (we recommend, however, using eq 3 for *D*(Au–Au) and the Perreault relation for *k*_e(Au–

(34) Huber, K. P.; Herzberg, G. *Molecular Spectra and molecular structure IV: Constants of diatomic molecules*; Van Nostrand: New York, 1979.

(35) (a) Schmidbaur, H.; Graf, W.; Müller, G. *Angew. Chem., Int. Ed. Engl.* **1988**, *27*, 417. (b) Narayanaswamy, R.; Young, M. A.; Parkhurst, E.; Ouellette, M.; Kerr, M. E.; Ho, D. M.; Elder, R. C.; Bruce, A. E.; Bruce, M. R. *Inorg. Chem.* **1993**, *32*, 2506. (c) Harwell, D. E.; Mortimer, M. D.; Knobler, C. B.; Anet, F. A. L.; Hawthorne, M. F. *J. Am. Chem. Soc.* **1996**, *118*, 2679.

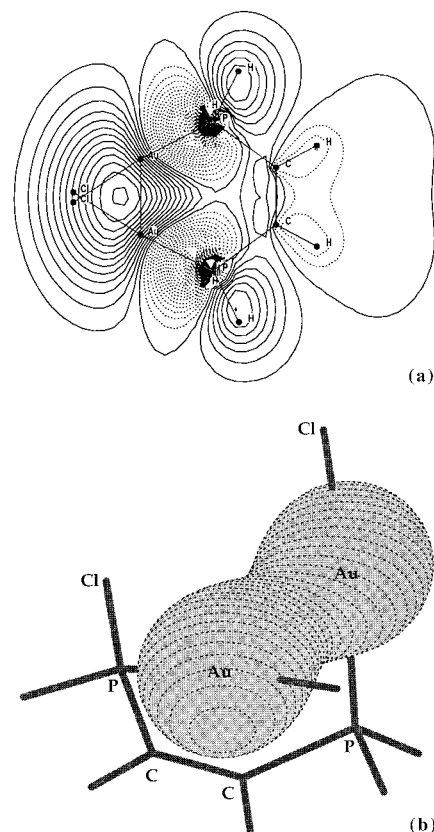


Figure 5. (a) Contour representation of the occupied MO responsible for the Au(6s) overlap in Au₂Cl₂C₂H₂(PH₂)₂. (b) Corresponding density plot showing the Au(s) contributions only.

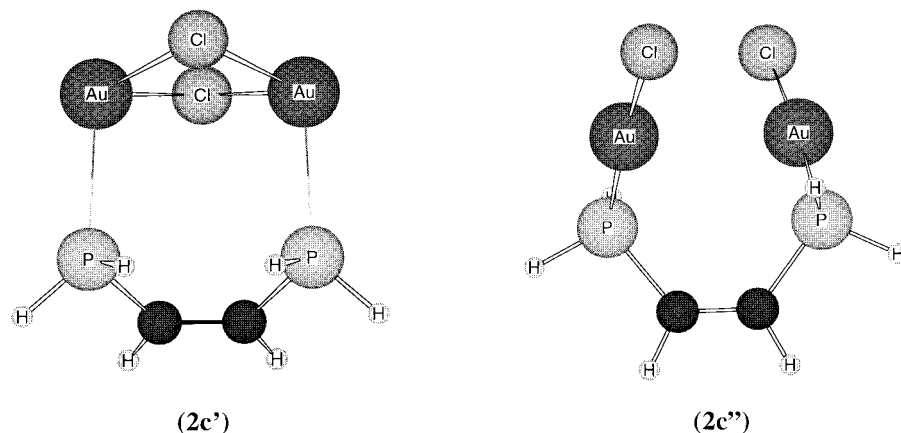


Figure 6. Optimized structures for $\text{Au}_2\text{Cl}_2\text{C}_2\text{H}_2(\text{PH}_2)_2$ at the nonrelativistic MP2 level ($2c'$) and the relativistic HF level ($2c''$).

Table 4. Mulliken Population Analyses and Dipole Moments for $\text{Au}_2\text{X}_2\text{C}_2\text{H}_2(\text{PH}_2)_2$ (X = Cl, Br, I)^a

property	$\text{Au}_2\text{Cl}_2\text{C}_2\text{H}_2(\text{PH}_2)_2$		$\text{Au}_2\text{Br}_2\text{C}_2\text{H}_2(\text{PH}_2)_2$		$\text{Au}_2\text{I}_2\text{C}_2\text{H}_2(\text{PH}_2)_2$	
	cis	trans	cis	trans	cis	trans
gross atomic charges						
Au	-0.18	-0.24	-0.08	-0.16	-0.16	-0.24
X	-0.24	-0.23	-0.34	-0.32	-0.25	-0.23
P	0.37	0.42	0.37	0.43	0.36	0.42
C	-0.33	-0.34	-0.32	-0.35	-0.32	-0.34
H _C	0.07	0.06	0.07	0.06	0.07	0.06
H _P	0.23	0.27	0.23	0.27	0.23	0.27
Au orbital populations						
6s	1.17	1.09	1.19	1.11	1.22	1.12
6p	0.18	0.32	0.17	0.29	0.18	0.29
6p _⊥	0.14	0.07	0.10	0.06	0.09	0.06
5d	7.71	7.82	7.64	7.75	7.69	7.81
5d _⊥	1.98	1.95	1.97	1.95	1.98	1.96
dipole moments	12.4	0	12.4	0	12.1	0

^a Dipole moments in D. The parallel || (perpendicular ⊥) component of the 5d and 6p orbitals represents the orbital components lying in (perpendicular to) the Au_2P_2 plane.

Au)). In any event, at 3.158 Å for $\text{Au}_2\text{Cl}_2\text{C}_2\text{H}_2(\text{PH}_2)_2$, we obtain $D(\text{Au}-\text{Au}) = 20$ kJ/mol, which is of the correct magnitude.

Weak auophilic interactions are probably difficult to analyze in terms of overlap or population arguments since these are mainly dispersive interactions.¹¹ Nevertheless, Figure 5 shows a contour plot of the occupied MO containing a clear bonding 6s overlap between the two gold atoms. This is also seen in the density plot of this MO where all other orbitals except the Au(s) orbital are neglected.

To investigate the importance of relativistic and electron correlation effects to auophilic interactions along the same lines as published earlier by Pyykkö et al.,⁹ we performed nonrelativistic MP2 and relativistic HF calculations for $\text{Au}_2\text{Cl}_2\text{C}_2\text{H}_2(\text{PH}_2)_2$. The structures are shown in Figure 6.

When electron correlation is neglected, the Au-Au bond distance increases to 4.68 Å (compound $2c''$ in Figure 6), a clear indication for dispersive-type interactions. On the other hand, if relativistic effects are neglected, we get quite a different compound which is best described as Au_2Cl_2 weakly interacting with the $\text{C}_2\text{H}_2(\text{PH}_2)_2$ ligand (compound $2c'$ in Figure 6). In this case, the Au-P bond distance increases from 2.28 to 4.43 Å! This clearly demonstrates that auophilic interactions are described by an interplay of relativistic and electron correlation effects.¹¹

It has been pointed out earlier that phosphine coordination to gold increases the Au-Au interaction which is enhanced by relativistic effects.²³ Considering reaction 1, $\text{Au}_2\text{X}_2\text{C}_2\text{H}_2(\text{PH}_2)_2 \rightarrow \text{Au}_2\text{X}_2 + \text{C}_2\text{H}_2\text{PH}_2$, we see that the decomposition energy

(ΔU) is relativistically increased from 93 to 333 kJ/mol for X = Cl; thus, $\text{Au}_2\text{X}_2\text{C}_2\text{H}_2(\text{PH}_2)_2$ is relativistically stabilized. Interestingly, ΔU decreases along the series X = Cl > X = Br > X = I. This trend is unchanged if we add the dimerization energies for the Au_2X_2 compounds, Table 5. This leads to the conclusion that the Au-P bond stability decreases along the series X = Cl > Br > I. Table 4 shows the Mulliken population analyses for the gold atom in $\text{Au}_2\text{X}_2\text{C}_2\text{H}_2(\text{PH}_2)_2$. As expected, we see Au(5d) participation in the gold-ligand binding as well as a nonnegligible Au(6p) population. In contrast, the Au(5d) participation in the Au-X bonding for Au_2X_2 is smaller, Table 5. It was pointed out earlier that phosphine coordination activates the Au(5d) electrons.²³ We should also mention that Rösch emphasized the importance of the phosphine substituents, L, to the Au-P bond stability in phosphine complexes of gold (e.g., RAuPL_3).³⁶ For example, density functional calculations show that substitution of the phenyl ligand by hydrogen atoms in $\text{CH}_3\text{AuPPh}_3$ diminishes the Au-P bond stability from 246 to 182 kJ/mol. Thus, our decomposition energies (ΔU) for reaction 1 are probably underestimated.

Excited-State Calculations for $\text{Au}_2\text{X}_2\text{C}_2\text{H}_2(\text{PH}_2)_2$. The first few CIS singlet excitation energies and the first singlet CAS-LMP2 excitation energies for the *cis*- and *trans*- $\text{Au}_2\text{X}_2\text{C}_2\text{H}_2(\text{PH}_2)_2$ compounds are shown in Table 6. We point out several important trends and features. All calculations show that the *cis* compound absorbs at a longer wavelength than the corresponding *trans* compound. The CIS procedure underestimates

(36) Häberlen, O.; Rösch, N. *J. Phys. Chem.* **1993**, *97*, 4970.

Table 5. Molecular Properties for Au₂X₂ (X = Cl, Br, I)^a

property	NR		AuCl	Au ₂ Cl ₂	AuBr	Au ₂ Br ₂	AuI	Au ₂ I ₂
	AuCl	Au ₂ Cl ₂						
distances								
AuX	2.475	2.688	2.288	2.540	2.404	2.635	2.580	2.787
Au–Au		3.364		2.779		2.762		2.758
X–X		4.194		4.252		4.487		4.845
angles								
Au–Au–X		51.3		56.8		58.4		60.4
energies								
ΔU		175.7		134.1		151.0		172.0
dipole moments	7.61	0	4.86	0	4.58	0	3.99	0
Mulliken populations and charges								
q(Au)	0.56	0.54	0.21	0.28	0.29	0.32	0.19	0.23
6s	0.26	0.26	0.66	0.61	0.70	0.69	0.74	0.76
6p	0.16	0.19	0.21	0.19	0.16	0.15	0.16	0.16
5d	10.02	10.01	9.91	9.86	9.86	9.87	9.90	9.85
frequencies (D _{2h} symmetry)								
A _g		46 (0)		95 (0)		95 (0)		91 (0)
B _{3u}		51 (19)		68 (6)		48 (2)		40 (1)
B _{3g}		140 (0)		101 (0)		90 (0)		88 (0)
B _{1u}		161 (59)		105 (50)		178 (32)		155 (23)
B _{2u}		210 (52)		246 (56)		76 (20)		68 (9)
A _g	290 (29)	228 (0)	349 (18)	285 (0)	242 (9)	198 (0)	196 (4)	165 (0)

^a Distances in Å, angles in deg, the energy difference ΔU for the Au₂X₂ → 2AuX dissociation in kJ/mol, dipole moments in D, Mulliken charges and orbital populations for Au in Au₂X₂, harmonic frequencies in cm⁻¹ (IR intensities in km/mol are set in parentheses). The stretching frequency for diatomic AuX is listed as well.

Table 6. First Three Singlet Vertical Excitation Energies for Au₂X₂C₂H₂(PH₂)₂^a

excited state	method	cis	trans	cis + 180°
X = Cl, 2				
1	CIS	215	179	189
	CASSCF	229	217	209
	CAS-LMP2	263	215	184
2	CIS	194	179	184
3	CIS	185	179	183
X = Br, 3				
1	CIS	216	195	200
	CASSCF	250	232	214
	CAS-LMP2	269	245	227
2	CIS	200	195	199
3	CIS	197	194	198
X = I, 4				
1	CIS	225	215	222
	CASSCF	263	253	276
	CAS-LMP2	312	245	235
2	CIS	216	215	222
3	CIS	216	215	220

^a All values are given in nm (10⁻⁹ m). All calculations are carried out at the optimized MP2 structure. cis + 180° denotes that the calculation has been carried out at an increased C=C–P–Au torsion angle of 180° (see Figure 8).

this effect. However, one clearly obtains the following trend in the wavelengths (λ) of the different halide species: λ(*cis*-Au₂I₂C₂H₂(PH₂)₂) > λ(*cis*-Au₂Br₂C₂H₂(PH₂)₂) > λ(*cis*-Au₂Cl₂C₂H₂(PH₂)₂). A similar trend but less significant is calculated for the trans species. These trends are consistent with the experimental absorption spectra for *cis*- and *trans*-Au₂X₂(dppe). The CIS calculations for *cis*-Au₂X₂C₂H₂(PH₂)₂ show that the next excited singlet states come at much lower wavelengths. As indicated in the Computational Details section, for *cis*-Au₂Cl₂C₂H₂(PH₂)₂, we succeeded in converging the CASSCF for the second excited singlet state. The CASSCF value is 207 nm compared to 229 nm for the first excited singlet state, and the CAS-LMP2 value is 212 nm compared to 263 nm for the first excited singlet state. This indicates that the *first* excited

state undergoes a large red shift. A comparison between the CIS and the CAS-LMP2 procedure also shows the limitations of a single reference CIS procedure. Indeed, the CI coefficients obtained from the CIS procedure all show a very strong mixing between a number of different states, in contrast to the simple C₂H₂(PH₂)₂ ligand. An analysis of the oscillator strengths at the CIS level shows a strong increase for the first excited singlet state when going from the trans to the cis structure. For example, for Au₂I₂C₂H₂(PH₂)₂, we obtain *f* = 0.13 for the trans and *f* = 0.20 for the cis conformations. The second excited singlet state for *cis*-Au₂I₂C₂H₂(PH₂)₂ gives a CIS oscillator strength of only 0.002. However, CIS oscillator strengths have to be taken with care, and for the ligand C₂H₂(PH₂)₂, they show very strong dependency on the basis set used. However, the trend is obvious, indicating that the red shift mentioned above is also accompanied by an increase in the oscillator strength.

Driving Force for Photochemical Cis-to-Trans Isomerization. An analysis of the CI coefficients shows a large C=C π* contribution from the ethylene unit in the first excited singlet state. We did not find any significant π* contributions in the first six excited singlet states of any of the *trans*-Au₂X₂C₂H₂(PH₂)₂ compounds! Density plots of the MOs for both the cis and the trans compound which contribute mainly to the first singlet excitation are shown in Figure 7. For both the trans and the cis compound, the first few singlet excitations can be best described by moving an electron out of a halogen lone-pair orbital, Figure 7a and 7c, and into a combination of Au(5d6s6p) orbitals with strong admixtures from a variety of other orbitals such as the phosphorus p orbital (and the ethylene π* for the cis compound), Figure 7b and 7d. However, the important unoccupied orbital shows no π* contribution in the trans structure (Figure 7b), in contrast to the cis compound which is mainly ethylene π* (Figure 7d).

To investigate the nature of the first few singlet excited states in more detail, we performed CIS calculations on *cis*-Au₂Cl₂C₂H₂(PH₂)₂ at different intranuclear Au–Au distances by rotating out one of the AuCl units. The corresponding singlet excitation energies depend on the C=C–P–Au torsion angle

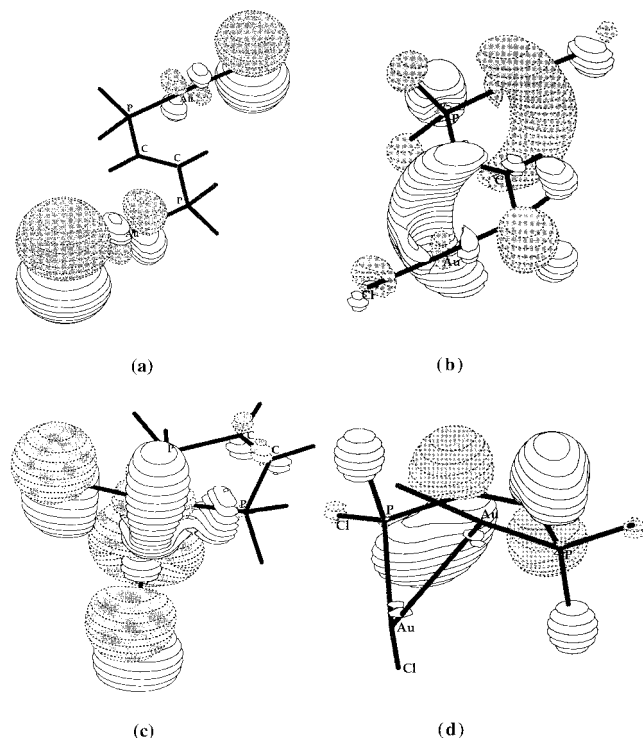


Figure 7. MO density plots showing the main orbital contributions for the first singlet excitation of *trans*- and *cis*- $\text{Au}_2\text{Cl}_2\text{C}_2\text{H}_2(\text{PH}_2)_2$. (a) Occupied MO for the *trans* structure showing one set of the chlorine lone pairs. (b) Unoccupied MO for the *trans* structure which mainly contributes to the first excited singlet state. (c) Occupied MO for the *cis* structure showing one set of the chlorine lone pairs. (d) Unoccupied MO for the *cis* structure (mainly $\text{C}=\text{C} \pi^*$).

(τ) as shown in Figure 8. Figure 8 also shows the Au—Au distance as a function of the $\text{C}=\text{C}-\text{P}-\text{Au}$ torsion angle.

At a torsion angle of about 180° , the Au—Au distance is ca. 5.5 \AA and the first three excited singlet states are very close in energy, as is also the case for the *trans* species. However, at smaller Au—Au distances starting at about 5 \AA , the first excited singlet state becomes significantly stabilized. The other two singlet states follow only at a much smaller Au—Au distance of about 3.5 \AA . This is also the case for the other halides as CIS calculations at an increased $\text{C}=\text{C}-\text{P}-\text{Au}$ torsion angle of 180° show, Table 6. We may therefore conclude that auriphilic effects (or at least close Au—Au contacts) stabilize significantly the first excited singlet state, thus leading to a red shift in the spectrum. This agrees with experimental observation and is schematically shown in Figure 9.⁵ A shift of electron density into the $\text{Au}(5d6s6p)$ orbitals upon excitation also points to an increase in the Au—Au interaction, which, however, could be in the repulsive region of the excited-state potential energy surface because of the energetically dominant $\text{C}=\text{C} \pi^*$ contribution. Since we underestimate the auriphilic interaction in our calculation (the Au—Au distance in $\text{Au}_2\text{Cl}_2(\text{cis-dppe})$ is 0.11 \AA smaller compared to our calculated value), we underestimate the red shift in our calculation. This is indeed the case if we compare our CAS-LMP2 value of 263 nm with the experimental absorption spectrum.⁵ Furthermore, the phenyl ligands may also contribute to the singlet excited states which are neglected in our calculations. However, the nature of the first singlet excited state (π^* for the *cis* but not for the *trans* compound) and the large red shift due to the auriphilic interaction clearly explains why only a *cis*-to-*trans* conversion in $\text{Au}_2\text{Cl}_2(\text{dppe})$ is observed in the UV region at wavelengths greater than 220 nm , but not vice versa.

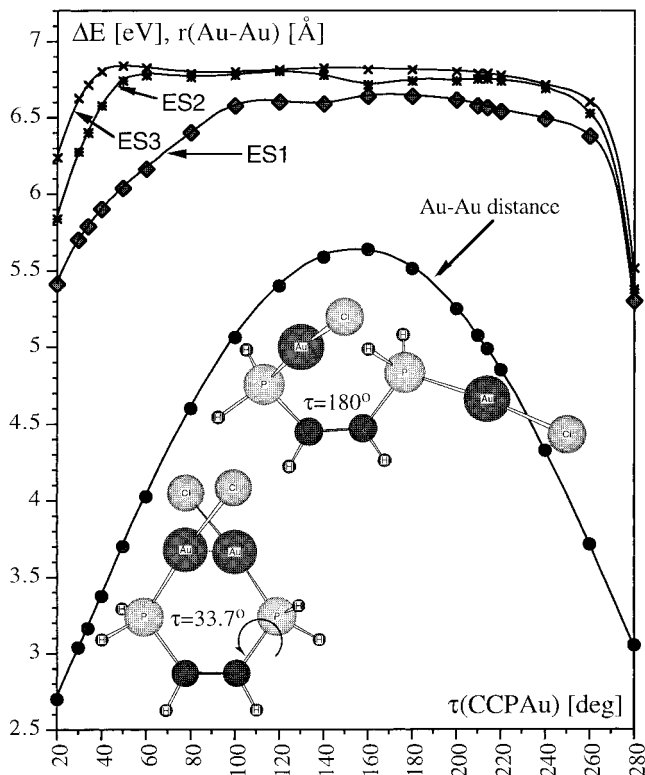


Figure 8. First three singlet excitation energies (in eV) and the Au—Au bond distance (in Å) as a function of the $\text{P}-\text{C}=\text{C}-\text{P}-\text{Au}$ torsional angle in $\text{Au}_2\text{Cl}_2\text{C}_2\text{H}_2(\text{PH}_2)_2$.

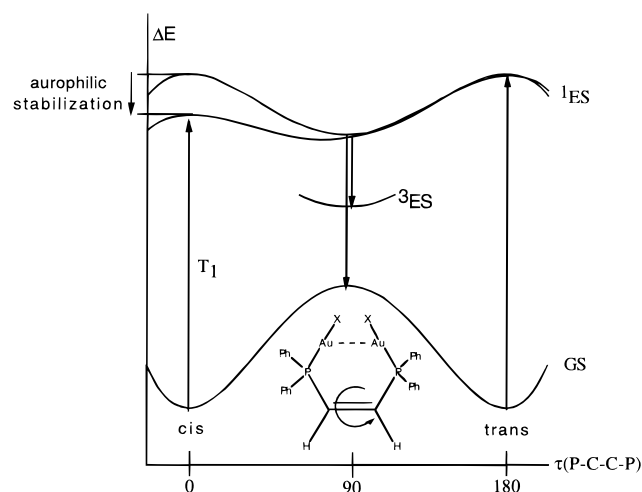


Figure 9. Schematic picture of the auriphilic stabilization of the first singlet excited state of $\text{Au}_2\text{Cl}_2\text{C}_2\text{H}_2(\text{PH}_2)_2$. GS denotes the ground state, ES the excited states, and T_1 the singlet transition. The multiplicities are given as superscripts.

We note that gas-phase AuCl emits at $19\,113.8 \text{ cm}^{-1}$ (523.2 nm)³⁷ and AuF at $17\,757 \text{ cm}^{-1}$ (563.2 nm).³⁸ Gas-phase AuBr and AuI have not been studied yet experimentally. Thus, complexation by phosphine significantly increases the excitation energy. One could argue that the halogen p orbitals become more diffuse when going to the heavier halides; thus, the HOMO orbital energy decreases going down the period. This leads to a decrease in the singlet excitation energy, as calculated, for example, for both *cis*- and *trans*- $\text{Au}_2\text{X}_2\text{C}_2\text{H}_2(\text{PH}_2)_2$. However,

(37) Wilkinson, P. G. *J. Mol. Spectrosc.* **1961**, *6*, 57.

(38) Saenger, K. L.; Sun, C. P. *Phys. Rev. A* **1992**, *46*, 670.

the calculations also show that the effect from the aurophilic stabilization to the first excited singlet state is by far more important.

Structures and Stability of Au₂X₂. There is not much known about gold halides in the gas phase, and we therefore briefly discuss the calculations on the gold halide dimers, Au₂X₂. The results of our calculations are shown in Table 5. The quality of the basis sets used in this work can be judged by comparing our MP2 bond distance for AuCl (2.288 Å) to results previously obtained with much larger basis sets (MP2, 2.211 Å; QCISD(T), 2.248 Å).³⁹ The results are in good agreement. Also, the relativistic bond contraction of 0.19 Å is in excellent agreement with previous MP2 (0.20 Å) or QCISD(T) results (0.19 Å). The vibrational harmonic frequency of 349 cm⁻¹ for AuCl also compares well with previous results (MP2, 384 cm⁻¹; QCISD(T), 361 cm⁻¹). The dipole moment (4.86 D), however, is overestimated (QCISD(T) value³⁹ is 4.05 D) since this property is more sensitive to basis set effects. This comparison gives an indication of the quality of the other properties predicted for AuBr and AuI.

As can be seen from the ΔU values for the decomposition Au₂X₂ → 2AuX, the stability of the dimeric gold halides, Au₂X₂, follows the trend Au₂F₂ < Au₂Cl₂ < Au₂Br₂ < Au₂I₂ (the ΔU value for Au₂F₂ of 100 kJ/mol is taken from ref 24). The trend in the Au–Au bond distance is interesting, Au₂F₂ (2.842 Å) > Au₂Cl₂ (2.779 Å) > Au₂Br₂ (2.762 Å) > Au₂I₂ (2.758 Å). This decreasing trend is *not* what one would expect from an increasing trend in the Au–X bond distance of the diatomic species; i.e., at the MP2 level, we obtain AuF 1.922 Å < AuCl 2.288 Å < AuBr 2.404 Å < AuI 2.580 Å. This interesting shortening of the Au–Au distance is in accordance with a widening of the Au–Au–X bond angle and points toward an aurophilic interaction in these compounds. If we compare with the nonrelativistically obtained MP2 Au–Au bond distances, we have 3.325 Å for Au₂F₂²⁴ and 3.364 Å for Au₂Cl₂. Hence, the decrease in the Au–Au distance is a relativistic effect, indicating again that aurophilic interactions become stronger with softer ligands. Since aurophilic interactions are dispersive interactions, they are difficult to interpret by overlap arguments and, indeed, the Mulliken population analysis does not reveal any positive overlap populations between the two gold atoms. Nevertheless, the Au₂X₂ species should be observed in the gas phase, and Table 5 includes the predicted harmonic vibrational frequencies and corresponding infrared intensities.

IV. Summary

Ab initio MP2 calculations were carried out on the *cis* and *trans* model compounds of Au₂X₂C₂H₂(PH₂)₂ (X = Cl, Br, I). Excited states were investigated by the CIS and CAS-LMP2 procedures. These calculations show the following important results:

(i) Aurophilic interactions in the *cis* compound increase with increasing softness of the ligand and are due to an interplay between relativistic and electron correlation effects. Nonrelativistic Au₂Cl₂C₂H₂(PH₂)₂ shows an unusual structure of C₂H₂(PH₂)₂ weakly bound to a Au₂Cl₂ unit.

(ii) Aurophilic interactions stabilize the first excited singlet state, thus leading to a red shift and increased transition moment in contrast to the *trans* product. This explains the unusual photochemistry observed in the UV region for these compounds.

(iii) The *cis* compound shows strong contribution from the π^* ethylene orbital in the excited state. Significant ethylene

π^* contributions have not been found in the first six excited singlet states of the *trans* isomer.

(iv) The stabilization of the first singlet excited state is critically dependent on the intranuclear Au–Au distance.

(v) The first few singlet excitations are best described by a charge transfer from a halogen lone pair into one of the Au orbitals with strong admixture of phosphorus p (and ethylene π^* for the *cis* species).

(vi) Further experimental work is required to evaluate the reason for the absence of photoisomerization for *cis*- and *trans*-dppee. We are currently conducting electrochemical studies to determine whether one-electron reduction (i.e., population of the LUMO) leads to isomerization.³¹ CIS calculations indicate π^* character in the first excited singlet state, but more accurate correlated calculations (like CASPT2) with larger basis sets may reveal a short-lived ethylene $\pi \rightarrow \pi^*$ excited state that rapidly relaxes to the lower energy phenyl $\pi \rightarrow \pi^*$ excited state, which is not photochemically active.

(vii) The Au–Au distance decreases in Au₂X₂ from X = F down to X = I despite the increasing Au–X bond distance along the same series of compounds. This again indicates some aurophilic interactions. The spectroscopic constants calculated for these compounds should help to identify these species in the gas phase.

The calculations were at the limit of our computer resources because of the overall large basis sets used in our calculations. We chose the MP2 procedure rather than the density functional approach in order to accurately describe dispersive-type aurophilic interactions. However, for obtaining excitation energies and transition moments of spectroscopic accuracy, much larger basis sets and a more sophisticated electron correlation procedure has to be applied, which is currently not feasible. We also note that gold is quite unique in showing strong aurophilic Au^I–Au^I interactions, which often is accompanied by photoluminescence behavior. For example, in a recent paper, Tzeng et al. synthesized [(LAu)(AuPPhMe₂)₂]₂ (H₃L = trithiocyanuric acid) which shows photoluminescence around 520–530 nm with long lifetimes of about 0.3 μ s.⁴⁰ These emissions are assigned to the sulfur lone-pair → Au excitation, similar to our case studied here.⁴¹ In the paper by Tzeng et al., it was also noted that aurophilic interactions cause a red shift in the UV region as found in our work. We believe that these aurophilic interactions may be the key to the understanding of the unusual photochemistry observed in gold compounds such as Au₂X₂(dppee), which is not detected for other group 11 metals.

Acknowledgment. P.S. is grateful to the Marsden fund Wellington (Contract Number 96-UOA-PSE-0081), the Royal Society of New Zealand, and the European Science Foundation (REHE program) for supporting this project. We thank the Auckland University Research and the High Performance Computer Committees for financial support and Prof. Pekka Pyykkö (Helsinki) for communicating his results on aurophilic interactions. We thank both referees for their critical comments.

JA973741H

(40) Tzeng, B.-C.; Che, C.-M.; Peng, S.-M. *J. Chem. Soc., Chem. Commun.* **1997**, 1771.

(41) Sulfur-to-Au CT excitations are also responsible for emission in a series of related gold(I) phosphine, thiolate complexes. See: (a) Jones, W. B.; Yuan, J.; Narayanaswamy, R.; Young, M. A.; Elder, R. C.; Bruce, A. E.; Bruce, M. R. M. *Inorg. Chem.* **1995**, *34*, 1996. (b) Forward, J. M.; Bohmann, D.; Fackler, J. P., Jr.; Staples, R. J. *Inorg. Chem.* **1995**, *34*, 6330.

(39) Schwerdtfeger, P. *Mol. Phys.* **1995**, *86*, 359.